Supplementary Materials: Realizations, Characterizations, and Manipulations of Two-Dimensional Electron Systems Floating above Superfluid Helium Surfaces

1. Electron emissions

Two-dimensional electron systems (2DESs) floating on helium surfaces are prepared by electron emission from a section of tungsten filament. The filament is soldered to a separate printed circuit board (PCB) which is placed at the central top, and its leads are wired to room temperature flange by copper wires with resistances about 1.5 Ω each. The resistance of the filament, measured at 1.0 K with a weak excitation current of 100 nA, is about 1 Ω. However, the resistance significantly increases to about 74 Ω when a current of 20 mA is applied. The resistance change is caused by the temperature rise due to Joule heating, and enables almost all heat dissipated on the filament instead of the copper wirings.

In order to prepare 2DESs, a voltage pulse was applied to the filament to trigger electron emissions at an environment temperature of about 1 K. The magnitude of the pulse was 1.55 V and its width was 20 ms. Smaller magnitudes or shorter pulses cannot trigger the emission well because filament temperature is not sufficiently high, while larger magnitudes or longer pulses will dissipate too much heat, which might cause violent evaporation of helium that destroys the helium surface. Preparations have been tested also at other temperatures. We also successfully prepared 2DESs at 1.5 K, but failed at 1.9 K and 0.3 K. The success at intermediate temperature suggests that vapor pressure of helium plays an important role: a high vapor pressure dissipates heat quickly from the filament, preventing it from reaching the threshold temperature and leading to violent evaporation of helium; while a low vapor pressure cannot effectively decelerate the electrons, with most of them penetrating the helium layer and drained through the electrodes.

2. Saturated electron density

The saturated electron density is determined by the potential well (as long as it does not trigger instability of helium surface), which is therefore dependent on the bias voltage V_0 applied to the three panel electrodes during the electron emission. Ideally, the 2DESs with sufficient density screen the electric field exerted by the electrodes and switch the flying electrons from acceleration to deceleration. Therefore, the as-grown 2DESs are at an electric potential very close to zero since its capacitance to the ceiling and rest walls is negligibly small compared with that to the panel electrodes. The electron density is given by $n_{as-grown} = \frac{\epsilon\epsilon_0 V_0}{ed}$.

Before conducting each transport measurement, the gate voltage V_{gate} was firstly swept negatively until the current vanished and a positive sweep was then started. During the initial negative sweep, the potential in the gate area was raised, and some electrons are expelled. This part of electrons either leave the helium surface or move out of the guarded area. They do not participate the transport measurements, and the saturating density determined by the transport window is approximately $n_s = \frac{2}{3} n_{as-grown} = \frac{2\epsilon\epsilon_0 V_0}{3ed}$.

3. Simulations of electron distributions

The quantity of electrons floating above helium surface is conserved during the transport measurements, but their distribution can be variable. To maintain the equilibrium of chemical potential within the plane, the local density of electrons above each electrode is associated with the voltages applied underneath. We hereby simulate the density variation along the longitudinal direction and its dependence on the gate voltage V_{gate}.

We simplify the simulation by assuming the existence of homogeneity in the transverse direction (defined as y direction as shown in Figure S1(a)). The potential profile in the $x - z$ plane can be given by Poisson's equation:

$$\frac{\partial \varphi^2}{\partial^2 x} + \frac{\partial \varphi^2}{\partial^2 z} = 0$$

where $\varphi(x, z)$ is electric potential. Two boundary conditions should be applied: (1) φ is determined by the biased voltages applied to the panel and guard electrodes at the bottom of the helium layer (see Fig. S1(b)); (2) φ remains at a constant value φ_0 at the top surface for static equilibrium of electrons. $\varphi_0 \geq 0$ and its specific value is related with the electron density n, which can be determined experimentally. With the numeric solution of the equation, the electric field normal to the helium surface can be determined by $E_{He}(x) = -\frac{\partial \varphi(x,z)}{\partial z}$, and the electron density can be given by $n(x) = -\left(\frac{\epsilon_0}{e}\right)[E_{vac}(x) - \epsilon E_{He}(x)]$. Here $E_{He}(x)$ and $E_{vac}(x)$ are the z components of the electric field underneath and above the 2DES, respectively. For our case, the 2DES strongly screens the field exerted by the panel electrodes, making E_{vac} negligible. Therefore, $n(x) = \left(\frac{\epsilon\epsilon_0}{e}\right)E_{He}(x) = -\left(\frac{\epsilon\epsilon_0}{e}\right)\frac{\partial \varphi(x,z)}{\partial z}$. We can see in Fig. S1(c) that the electrons can be effectively manipulated by variating the voltage on the gate electrode, from depletion to accumulation of almost all electrons. The local density in the gate area is proportional to V_g at least for $V_g < 25$ V (see Fig. S1(d)).

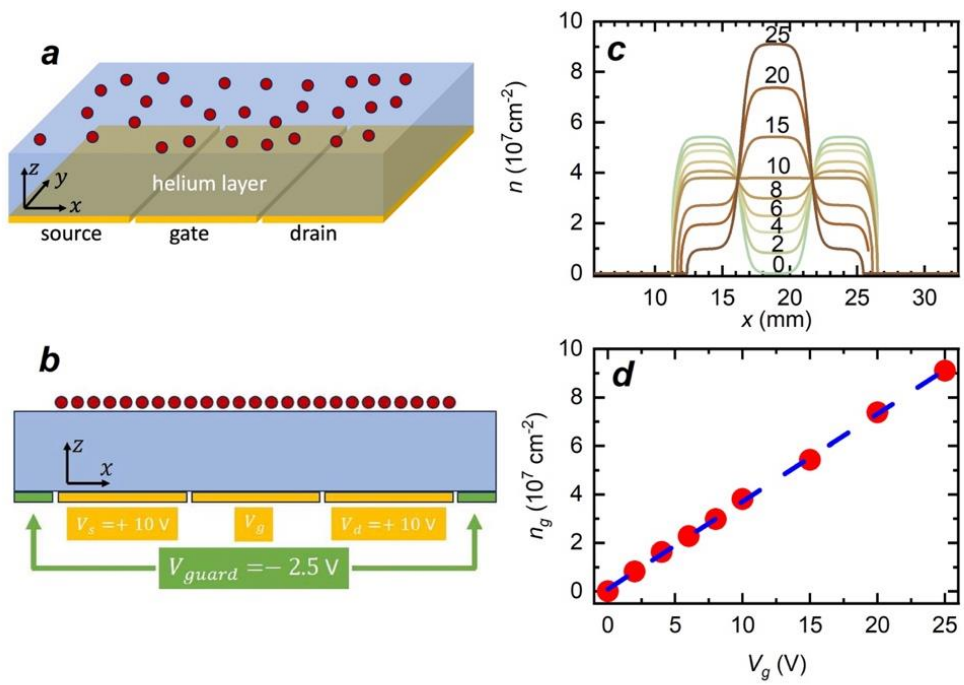

Figure S 1 (a) Schematic drawing of a 2DES floating on helium surface. (b) Side view of the schematic drawing in panel (a) for numeric simulations. The bias voltage on the guard electrode is set at -2.5 V, and those on the source and drain electrodes are set at +10 V. The voltage of the gate electrode is tuned with various values in order to demonstrate the manipulation of electron distribution. (c) Electron density along the longitudinal direction simulated with multiple gate voltages (indicated by the labels next to each curve). (d) Linear dependence of the electron density in the gate area n_g on gate voltage V_g.

4. Transmission-line model

The model treats 2DESs as transmission lines of electron motion which are capacitively coupled to the electrodes. For the specific geometry of our experimental setup, the transmitted current detected by the drain electrode is dependent on the effective two-dimensional conductivity of the 2DES (σ) and angular frequency (ω), as given by eqn. (1) in the main text. Figure S2 exhibits the calculated dependence of current on σ and $f = \omega/2\pi$. A clear onset transition is displayed by both imaginary and real components of current as σ increases, and the transition shifts to higher critical value of σ at higher frequency. This is in qualitative consistence with our observation of the transition shifting to higher V_{gate} as more electrons enter the gate area to increase the effective σ.

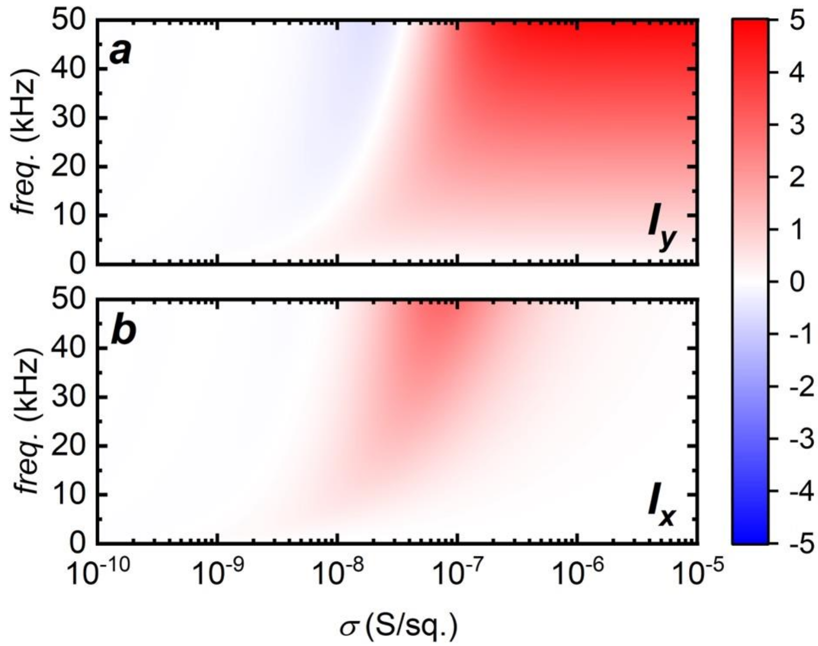

Figure S 2 Dependence on frequency and two-dimensional conductivity for the imaginary (a) and real (b) component of current. The plot is calculated based on eqn. (1) in the main text.

5. Simulation of potential field and fringing effect

Potential profiles 1 mm and 0.1 mm above the electrodes are simulated respectively by Finite-element modelling (FEM) and presented in Fig. S3. Obvious blur can be seen for the layer 1 mm above the surface. It is clear that fringing effect can be efficiently suppressed by reducing the distance from the electrodes to the layer.

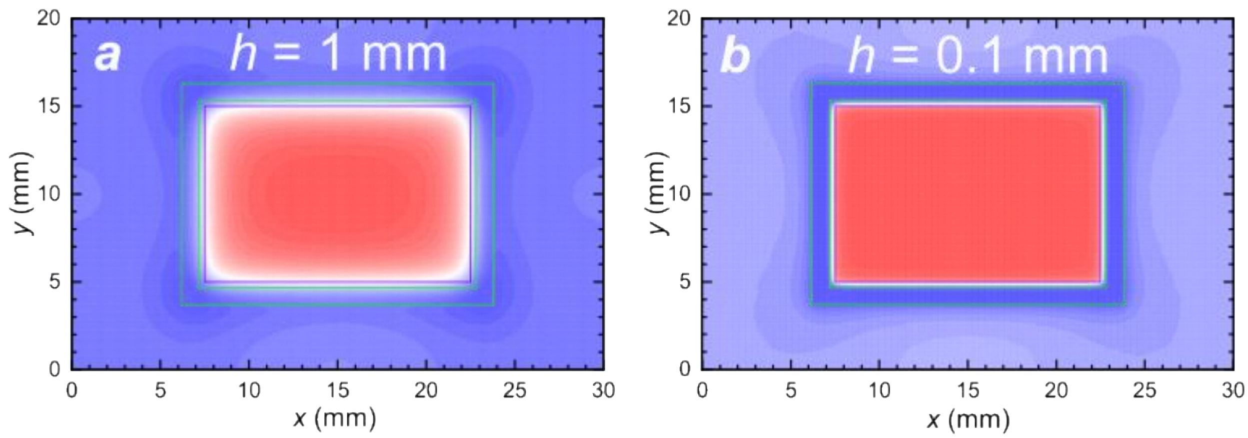

Figure S 3 Potential profile of the layer at the height of 1 mm (a) and 0.1 mm (b) above the electrodes. For simplicity, the three panel electrodes are combined into one piece. V_0 is set at +10 V and V_{guard} at -2.5 V. The purple and green lines depict the area of the panel and guard electrodes, respectively. The potential is positive in the red area and negative in the blue area.